Quarterly Technical Progress Report

Fourth Report
April 16, 2000 –July 15, 2000

Title: *A Novel CO_2 Separation System*

Contractor: TDA Research, Inc.
12345 W. 52nd Avenue
Wheat Ridge, CO 80033

Principal Investigator: Robert J. Copeland

Sponsor: U.S. Department of Energy

Contract DE-AC26-98FT40421--04

Technical Monitor: Thomas P. Dorchak
Project Manager
National Energy Technology Lab
U.S. Department of Energy
3610 Collins Ferry Road
P.O. Box 880
Morgantown, WV 26507-0880

Reporting Period: **April 16, 2000 –July 15, 2000**

PROJECT DESCRIPTION

Introduction

Because of concern over global climate change, new systems are needed that produce electricity from fossil fuels and emit less CO_2. The fundamental problem with current systems that recover and concentrate CO_2 from flue gases is the need to separate dilute CO_2 and pressurize it to roughly 35 atm for storage or sequestration. This is an energy intensive process that can reduce plant efficiency by 9-37% and double the cost of electricity.

There are two fundamental reasons for the current high costs of power consumption, CO_2 removal, and concentration systems: 1) most disposal, storage and sequestering systems require high pressure CO_2 (at roughly 35 atm). Thus, assuming 90% removal of the CO_2 from a typical atmospheric pressure flue gas that contains 10% CO_2, the CO_2 is essentially being compressed from 0.01 atm to 35 atm (a pressure ratio of 3,500). This is a very energy intensive process. 2) The absorption-based (amine) separation processes that remove the CO_2 from the flue gas and compress it to 1 atm consume approximately 10 times more energy than the theoretical work of compression because they are heat driven cycles working over a very low temperature difference. Thus, to avoid the problems of current systems, we need a power cycle in which the CO_2 produced by the oxidation of the fuel is not diluted with a large excess of nitrogen, a power cycle which would allow us to eliminate the very inefficient thermally driven absorption/desorption step. In addition, we would want the CO_2 to be naturally available at high pressure (approximately 3 to 6 atmospheres), which would allow us to greatly reduce the compression ratio between generation and storage (from roughly 3,500 to approximately 8).

To meet this objective, we propose a power generation system in which a fossil fuel (gasified coal, petroleum fuels or natural gas) at pressure is used to reduce a metal oxide, producing metal (or a lower valance metal oxide), CO_2 and water (Figure 1). The water is condensed and its energy used to raise steam, leaving behind a stream of pure CO_2 at 3 to 6 atmospheres that can be readily stored or sequestered. The metal oxide is then "burned" or re-oxidized in air from the compressor section of a gas turbine, producing a hot high-pressure stream of air that is used to drive a gas turbine. The exhaust can in turn be used to drive a steam bottoming cycle. The oxidized particles are then recycled to the first reactor to be reduced again and repeat the cycle. The system that transfers the energy of the fuel to the air without bringing the carbon along is called a Sorbent Energy Transfer System (SETS). The cycle can be run on any fuel gas (gasified coal, oil or natural gas) and does not require the development of new hardware. The power generation cycle is essentially a standard combined cycle, except that the combustor is replaced by two fluidized beds (the SETS): one that uses fuel to reduce the particulate oxide and one that oxidizes it and heats the air entering the turbine. The system is described below using methane as the fuel (because it is simplest to explain).

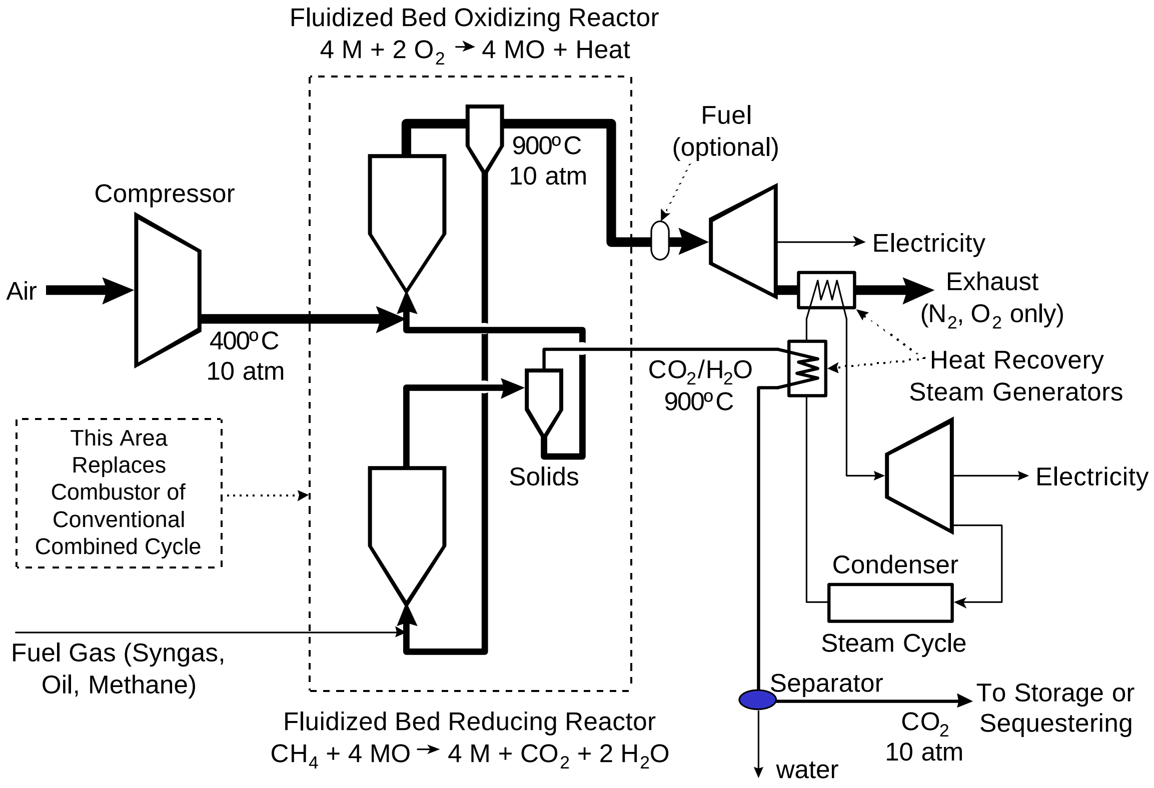

Figure 1. Sorbent energy transfer cycle schematic (M = metal).

The first step in the SETS process is to reduce a metal oxide to a metal (or a metal oxide to a lower valance metal oxide). In general, the metal (oxygen sorbent) would be supported on, or contained within, an inert support (such as alumina) that would provide a high surface area for reaction and good physical properties such as crush strength and attrition resistance. For example, if copper were the metal oxide the formula would be:

$$CH_4 + 4\ CuO \rightarrow CO_2 + 2\ H_2O + 4\ Cu$$

In this way, we convert the energy in the fuel to energy that is stored in the reduced metal, and produce a stream consisting of 33% CO_2 and water. We carry this out at pressure (10 atmospheres, for example) in a fluidized bed reactor, and remove the steam from the CO_2 by condensing it (producing valuable mid-pressure steam which can be used to generate electricity in the steam turbine of a combined cycle) and a stream of virtually 100% pure CO_2 at 10 atm. The CO_2 is sent to a storage or sequestering process with little additional compression energy.
Virtually all of the chemical energy in the original fuel gas is now incorporated in a new fuel (small particles of copper on an inert support). The reduced copper particles enter a second fluidized bed (also run at 10 atm) and are re-oxidized with air, producing large amounts of heat and heating the air to the temperatures needed to drive a gas turbine-combined cycle (900ºC or greater).

$$4\ Cu + 2\ O_2 \rightarrow 4\ CuO$$

The air entering the oxidizing bed is the hot (400°C) high-pressure (10 atm) air leaving the compressor stages of a standard gas turbine. The only CO_2 emissions from such a system would be produced if we burned some additional fuel to further boost the temperature of the high-pressure air just before it entered the expander stages of the turbine. The copper/alumina particles would then be returned to the reducing reactor and the cycle repeated.

This power cycle requires no new hardware; it is essentially a standard combined cycle in which the combustor is replaced by the fluidized bed oxidation and reduction reactors. The system can dramatically reduce or eliminate CO_2 emissions. The degree of CO_2 removal is limited only by the performance of the filters used to protect the turbine. With current 900°C filters the cycle would reduce the CO_2 emissions of a coal gasifier combined cycle by 83% while suffering only a 1.5 - 4% efficiency penalty. With the advanced filters currently under development, CO_2 emissions could be totally eliminated with no additional efficiency penalty. Since the power cycle uses only standard combined cycle generating equipment and two circulating fluidized bed reactors, the major research needs are further design, sorbent development, pilot scale testing and detailed engineering and cost analyses.

Geodes for a Long Life Sorbent

To make a sorbent pellet that can hold large amounts of sorbent without being destroyed by the absorption-regeneration process, TDA has developed a new sorbent structure, which we call a geode (Figure 2). Like the geode that you buy at a gift shop, our geode has a hollow shell. The sorbent is loosely contained in, but does not fill, the hole(s) in the center. Thus, the sorbent can expand and contract indefinitely without destroying the pellet structure that surrounds it. Unlike the gem shop geode that has a single hole in the middle, our geode sorbent contains hundreds or thousands of holes in a structure that looks like a conventional catalyst support pellet on the outside. The interior structure of the geode is like a sponge, a sponge that is partially filled with the chemically active material, copper and/or iron oxides.

To make the very small (e.g., 100 µ) particles required by fluidized bed and transport reactors, TDA has modified our previous methods of making the geode. We mix the active component of the sorbent with water, a low cost inert material, and other additives. The mixture is formed by spray drying or extruding and then firing. After firing, the water and some additives evaporate and/or burn, leaving behind a complex porous structure.

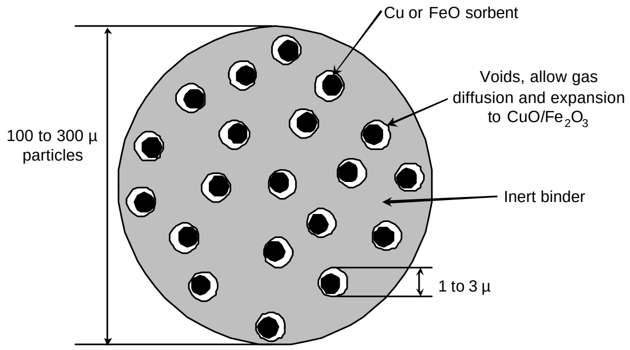

Figure 2. Structure of TDA's "geode."

Due to the nature of this mixture, it separates upon firing into two different phases which are each thermodynamically stable. Data from both published phase diagrams and our independent measurements show that the phases are physically separate. The size of each chemically active region of the geode (i.e., 1-3 µm) is controlled by the selection of the starting materials.

In the geode structure there are voids in both the mixed chemically active and inert phases. The binder is a continuous porous structure filled with extremely small pores (0.1 to 1 µm). This structure holds the sorbent in place. Because of the porosity left behind as the water evaporates, the O_2, H_2, and CO can easily diffuse in from the exterior of the pellet to the tiny pockets of sorbent. The geode structure: 1) is very strong because there is a continuous support phase, 2) effectively contains the sorbent inside small holes in the interior of the pellet, 3) allows the sorbent to expand and contract freely without disrupting the pellet structure, 4) allows the gases to diffuse quickly into the interior of the pellet, and 5) can hold large quantities of sorbent and absorb large quantities of oxygen. In addition, the process that we use to produce the geode is inherently low in cost. The geode is formed by mixed metal oxide techniques, yet it has the continuous inert structure associated with catalyst supports, which have high strength and long life.

TECHNICAL OBJECTIVES

The Phase I research will carry out preliminary proof of concept experiments to determine whether the geode structure can be used to make a low-cost, long life, redox metal oxide based sorbent for use in the SETS cycle. The specific goal of the Phase I work is to optimize the formulation of the geode in order to obtain the following properties:

- Less than 10 lbs of oxygen per 100 lbs of fresh sorbent,
- An 80 to 300 micron particle size,
- Reduction @ 700°C (1292°F) with oxidation initiated with 400°C (752°F) air, and
- Costs of less than $8/lb when produced at 50,000 lbs/year.

Technical Approach

In order to bring our new power cycle from a concept to a commercial reality we need a team with a variety of skills. Specifically, in this three phase program we need to:

1) Carry out the conceptual and thermodynamic analyses necessary to better define the cycle and optimize the reaction conditions,
2) Develop a sorbent with suitable physical and chemical properties,
3) Test the sorbent at the laboratory and pilot scale,
4) Engineer the oxidation and reduction reactors,
5) Prepare detailed engineering designs to predict the total cycle performance and cost.

To provide the necessary skills, we have assembled a team that includes TDA Research (TDA), M.W. Kellogg (Kellogg) and Louisiana State University (LSU) (Figure 3). TDA invented the new system design. TDA will manage the project, carry out the conceptual engineering and thermodynamic analysis to define the process, and develop the sorbent. Kellogg will review the initial conceptual designs, carry out detailed engineering analyses, and test the sorbent in their circulating fluidized bed pilot facility. LSU will aid in the thermodynamic analyses. Kellogg, one of the largest U.S. engineering and construction contractors (with particular experience in fluidized bed design and construction) has the ability to provide complete commercial scale facilities.

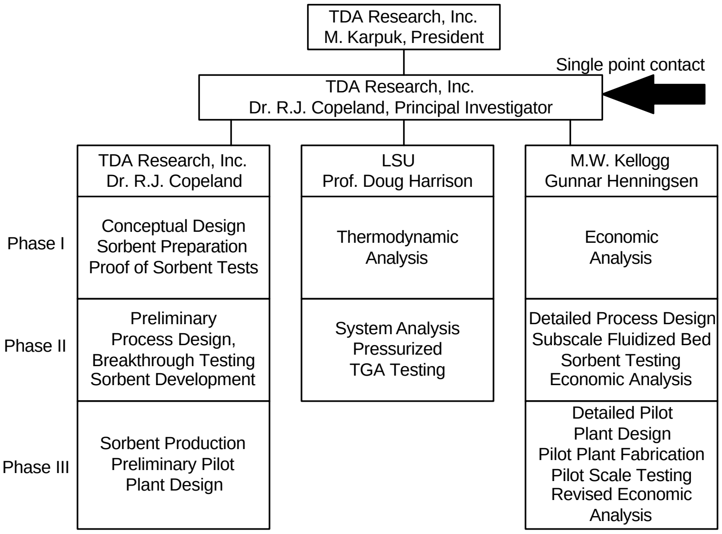

Figure 3. Project organization.

SUMMARY

During this quarter we focused on testing sorbents and identifying methods to maximize CO_2 capture with SETS. In June we found that sorbents that contained copper, even in small amounts, showed a tendency to agglomerate after a few cycles in our HTHP fluidized bed reactor. Therefore, our current testing is with copper-free sorbents.

We started doing 50 cycle tests on prospective sorbents to better understand their long-term behavior. We successfully tested the iron-based oxygen sorbent at $800^{o}C$, through 52 cycles, and it demonstrated consistent oxygen loadings. This sorbent is also very strong, measuring 0.67 on the attrition index (which implies a life of over 10 million cycles in a transport reactor) and, therefore, represents a very low sorbent replacement cost.

In an effort to increase oxygen loading and operating temperatures, we are preparing spray dried sorbents using nickel instead of iron.

We are investigating ways to improve CO_2 capture in the SETS. Tom George of DOE-NETL provided data on UltraFuelCell with gas turbine power cycles, which have conversion efficiencies of 80% (LHV) using natural gas. Using his data, we are evaluating the integration of SETS into the UltraFuelCell systems. With a high temperature SETS sorbent, our analysis indicates only a 2.3% loss of power for 100% capture of the CO_2 in a high temperature fuel cell system. Excluding the price of the SETS reactors and CO_2 compressors capable of 750 psia (51 atm), the cost is only ~$3.5 per ton of CO_2.

With the GE gas turbine combined cycle (GTCC), SETS adds $10.9 million (see LSU subcontract report No. 10 included herein). SETS also increases the heat rate of the combined cycle by ~4%. Including sorbent replacement, SETS adds 7.7% to the Cost Of Electricity (COE). This equals $14/ton of CO_2 captured in a GTCC.

Louisiana State University (LSU) examined two areas of interest during June. Changes were made in the base case simulations using both Cu-Fe and Fe-only sorbents to increase the sorbent circulation rates to 120% of stoichiometric (the previous sorbent circulation rate was 100% of stoichiometric). In addition, one standpipe was eliminated in the three-reactor configuration using Cu-Fe sorbent, and the diameters of the remaining standpipes were decreased. The first-round estimate of purchased equipment costs and total capital requirement for the Cu-Fe sorbent for the SETS process is $10.9 million, or just under 10% of the base total capital estimate for the GE MS7001FA natural gas combined cycle plant (Appendix A).

Sorbent tests results

Table 1. Simulated reactor conditions for fluidized Bed testing at TDA.

	GTCC Reduction	**Fuel Cell Reduction**
	(wet/dry) vol%	(wet/dry) vol%
CO_2	8.3 / 10.0	7.6 / 9.5
CH_4	8.3 / 10.0	-
H_2		7.2 / 9.0
CO		5.2 / 6.5
H_2O	16.7 / -	20.0 / -
N_2 Diluent	66.7 / 80.0	60.0 / 75.0
Temp.	775 – 875 (°C)	775 – 875 (°C)
Pressure	150 (psig)	150 (psig)
	GTCC Oxidation	**Fuel Cell Oxidation**
	vol%	vol%
O_2	2.0 – 5.0	2.0 – 5.0
N_2 Diluent	95.0 – 98.0	95.0 – 98.0
Temp.	775 – 885 (°C)	775 – 885 (°C)
Pressure	150 (psig)	150 (psig)

Sorbent screening in our modified HTHP fluidized bed reactor system is continuing. Several runs were conducted on prospective sorbents, using two different simulated gas compositions. Two types of sorbents (one with copper and iron and the other with iron only) were selected for initial screening from the materials that were spray dried at Coors Ceramics. The difference in the two was the presence of a small amount of copper oxide in one of the sorbents. The two different gas compositions (Table 1) reflect the initial SETS application in a Gas Turbine Combined Cycle (GTCC) and the gas mixture that would result from the presence of a proposed upstream fuel cell. The gas mixture may offer some advantages in the efficiency and cost of CO_2 capture, and in the reduced cost of capital equipment.

We selected materials to load into the HTHP fluidized bed based on their attrition resistance and on data gathered from TGA testing of all the proposed sorbents. The first material loaded was a composition containing just iron and alumina (No. 505000-1100.) This material has several advantages: it achieves the highest level of attrition resistance at the lowest firing temperature of all the sorbents tested; it is the simplest in construction, containing a minimal amount of different materials to order and store; the raw materials are the cheapest and most easily attainable; and its performance in the TGA is excellent. The results of the attrition tests, and the chemical compositions and calcination temperatures for the fabricated sorbents, are summarized in Table 2.

Table 2. Results of the air jet attrition test for synthesized sorbents.

Sorbent Composition	Firing Temperature, °C	Attrition Loss, wt% loss/h	Bulk Density, g/cc
5% CuO/45% Fe_2O_3/ Al_2O_3	950	19.89	1.63
	1050	8.82	1.74
	1200	1.30	2.03
50% Fe_2O_3 / Al_2O_3	950	15.98	1.59
	1050	8.81	1.77
	1100	5.45	1.91
	1200	0.64	2.17

The tests were done for a period of 2.5 hours. Fines generated in the first hour were included in the total loss calculations. The generally accepted attrition index (A.I.) value for use in a transport reactor is 5 wt% loss/h for the ASTM test protocol; we have found that this relates to a value somewhere around 12-13 wt% loss/h on our instrument.

The values presented in Table 2 should be considered representative of relative strengths rather then final values as, upon examination with a low power microscope, the spheroids formed from the test spray drying were dimpled (see Figure 4). This dimpling could be eliminated with some optimization of the processing step, which should also improve the strength of the resulting particulate.

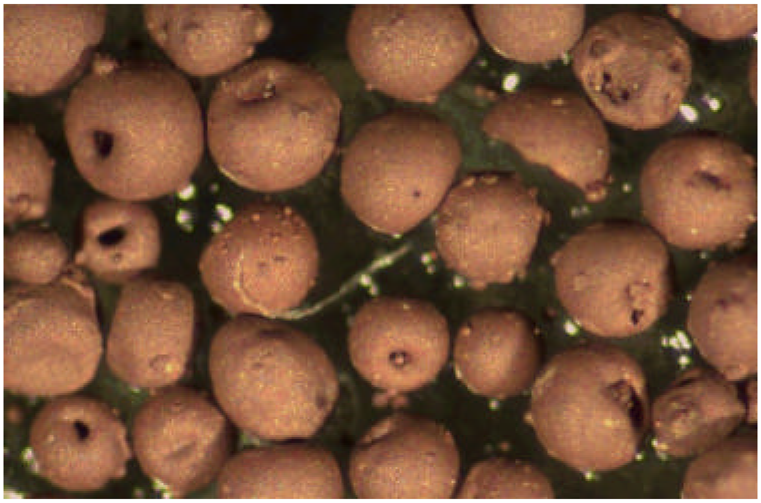

Figure 4. Example of dimpling on the test batches of spray-dried materials.

We estimated the life of these sorbents based on a comparison between these initial measurements and the measurements of another cycled sorbent. Under a DOE SBIR contract, TDA subcontracted to Norton Chemical Process Products (Norton) the fabrication of a zinc ferrite sorbent by techniques that were similar to large-scale production. Their sample number was Lot N9925548. Kellogg, Brown, & Root (KBR) tested that sorbent and measured the material against the Davison Index. We also measured the attrition index in our attrition tester. The TDA results are reported in Table 3. The zinc ferrite sorbent also had grape-like clusters and, therefore, a high attrition rate when it was fresh (our recently spray-dried sorbent has a similar problem). After cycling in KBR's TRTU, the attrition index improved (due to the removal of the grape-like clusters). KBR estimated that the long-term attrition rate of the N9925548 sorbent was only 0.55(10)$^{-6}$ lb/lb-circulated. TDA measured an attrition index of 9 for the new Cu sorbent using the same apparatus that measured Lot N9925548. Although the new Cu sorbent had a better attrition index when the material was fresh, the loss mechanisms could be different; we conservatively estimated that the loss rate of this material would be ~1(10)$^{-6}$ lb/lb-circulated.

Table 3. Extrapolation of attrition loss rate.

Sorbent identification	Lot N9925548	*New Cu sorbent*
Bulk density of fresh sorbent	82.4 lb/ft^3 (1.32 gm/cc)	*1.74 g/cc*
D_{50} after 5 cycles in MC test	115 µm	
D_{50} after 10 cycles in MC test	100 µm	
TDA attrition index for fresh[1]	17	*9 (@1050^{o}C)[2]*
TDA attrition index after 5 cycles in TRTU test[1]	11	
TDA attrition index after 10 cycles in TRTU test[1]	9	
		New iron based sorbent
Bulk density of fresh, iron based sorbent		*2.17 g/cc*
TDA attrition index for fresh[2]		*0.64 (@1200^{o}C)*

[1] Since sorbent has grape-like clusters, which rapidly attrite, the 10th cycle attrition index is more representative of the sorbent long-term attrition behavior.

[2] Dimpled spray dried sorbents

Long term attrition rate, Lot N9925548 lb/lb circulated	0.55x10^{-6}
Long term attrition rate, New Cu sorbent lb/lb circulated	*~1x10^{-6}*
New iron based sorbent lb/lb circulated	*~ 1x10^{-7} (or 10 million cycle life)*

For our 1200^{o}C fired, iron based sorbent the loss rates are substantially lower (a 0.67 attrition index, versus 9 for copper and 9 for the sorbent tested in the TRTU). The loss rate for the iron based sorbent was conservatively estimated as an order of magnitude lower than that of the copper or a loss rate of 1 (10)$^{-7}$ lb/lb circulated (a 10 million cycle life). Figure 5 shows a Scanning Electron Microscope (SEM) of this sorbent. The sorbent has continuous porosity that allows gases to easily diffuse into and out of the sorbent. The small particles are also jointed together, providing a continuous structure that gives this sorbent its low attrition index (high strength).

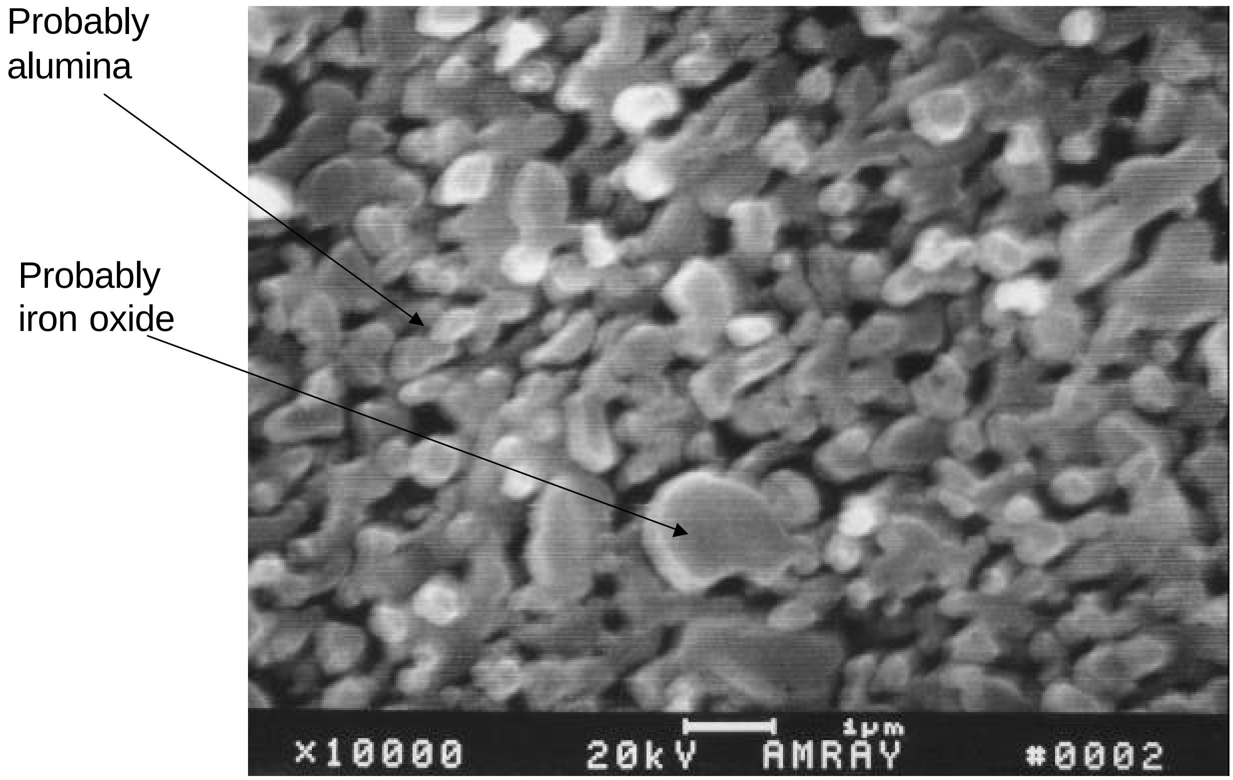

Figure 5. TDA Research spray dried iron based sorbent (1200°C) 10,000X SEM

Multiple Cycle Testing in a Fluidized Bed

Given the excellent attrition index for the 1200°C iron based sorbent, we conducted extensive tests with it. All tests were done in the simulated gas compositions detailed in Table 1, unless noted otherwise. The first test regime conducted on the 1200°C material was the typical fuel cell scenario using 825°C as the initiation point for both reduction and oxidation. The initial tests showed that the sorbent was indeed active, even with a 1200°C firing temperature, and was a viable candidate for continued exploration. We then increased the test conditions to simulate the higher temperature environment associated with an UltraFuelCell system. These tests showed that the iron sorbent, while a good performer at the lower operating ranges (800°C), had a tendency to agglomerate at higher operating conditions.

We then reloaded the HTHP fluidized bed reactor with 1200ºC fired iron-based sorbent for multiple-cycle testing at lower operating temperatures. The temperature chosen to initiate both reduction and oxidation was 720ºC, and the oxygen content for the oxidation cycle was such that the resulting exotherm would bring the bed to a final temperature of 800ºC (8.0 vol%). We conducted a 52 cycle test using an automatic sequence alternating between oxidation and reduction, triggered by either CO breakthrough (CO > 0.2% outlet) for reduction, or O_2 breakthrough (O_2 > 0.5% outlet) for oxidation. Each alternate cycle was separated by a N_2 purge. We have completed the planned 52 cycles, which are portrayed in Figure 6. As can be seen, the sorbent experienced an early deactivation, followed by a slow reactivation (an effect we have seen in other geodes).

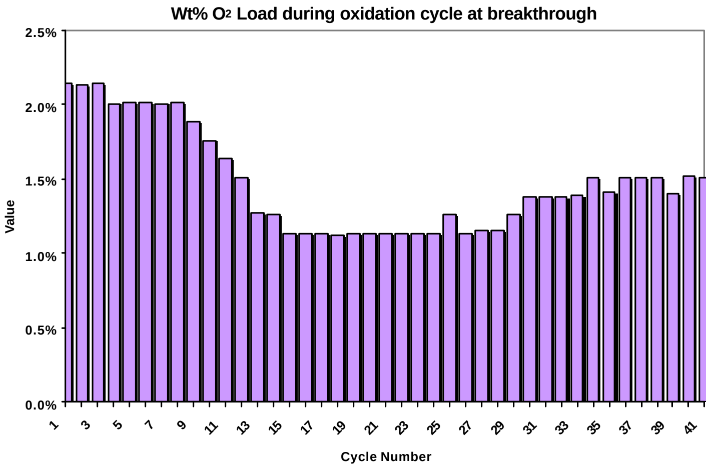

Figure 6 Multicycle O2 carrying capacity.

Figure 7 shows the difference between an early cycle reduction (cycle 2) and a later one (cycle 42). These differences can be characterized by the shape of the CO breakthrough (which is more gradual in cycle 42) and the duration of CO removal (which is shorter in cycle 42).

Because of the relatively low O_2 carrying capacity of iron (1 mole O_2 for 6 moles Fe_2O_3) and its limited operating temperature range, we are now focusing our research on sorbents containing nickel. Despite its high cost, nickel has several advantages over iron which should offset this cost differential: the O_2 carrying capacity of nickel is much higher than that of iron; it is a known reforming catalyst, which may offer some advantages in the SETS scenario with CH_4 in the inlet; and it has an operating temperature that is expected to be much higher than that of iron oxide. To this end, we have impregnated several alumina catalyst carriers with nickel and will be loading them in the HTHP reactor. Additionally, we have ordered the materials for a several bulk spray dryings of nickel-based sorbents.

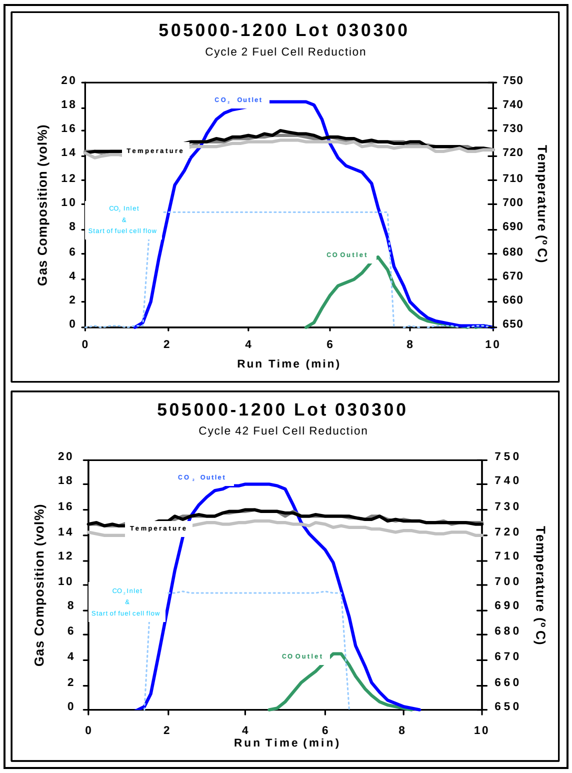

Figure 7 Early vs. late reduction cycles.

<u>Cost of SETS with Gas Turbine Combined Cycle</u>

With the GE gas turbine combined cycle, which has a turnkey cost of $114,900,000 (Gas Turbine World, 1999-2000 Handbook), SETS adds $10.9 million (see LSU subcontract report No. 10 included herein) for a total cost of $125,800,000. SETS also increases the heat rate of the combined cycle by ~4% (due to losses in efficiency from 55% to 53%). The combined effect of increased capital costs, decreased efficiency, and additional O&M (for added capital and sorbent replacement) adds 7.7% to the COE (i.e., $/kWh). This is equal to $14/ton of CO_2 captured.

100% CO_2 Capture with SETS

We are evaluating the potential for SETS to capture 100% of the CO_2 produced in the power plant and, based on input from DOE, are including a fuel cell in the combined cycle. We received a report on an *Advanced High Temperature Fuel cell System*, draft 1st Revision, April 25, 2000 from Tom George at DOE-NETL. A paper contained in that report by Robert E. James III, updated an earlier report by Robert E. James III and Tom J. George, “Economics of Scale Report: Multistaged, Solid State, Fuel cell Plant with Gas Turbine,” April 2000, that described an UltraFuelCell Power Plant with an 80% efficiency (LHV) with natural gas and without CO_2 capture. That system is shown in Figure 8.

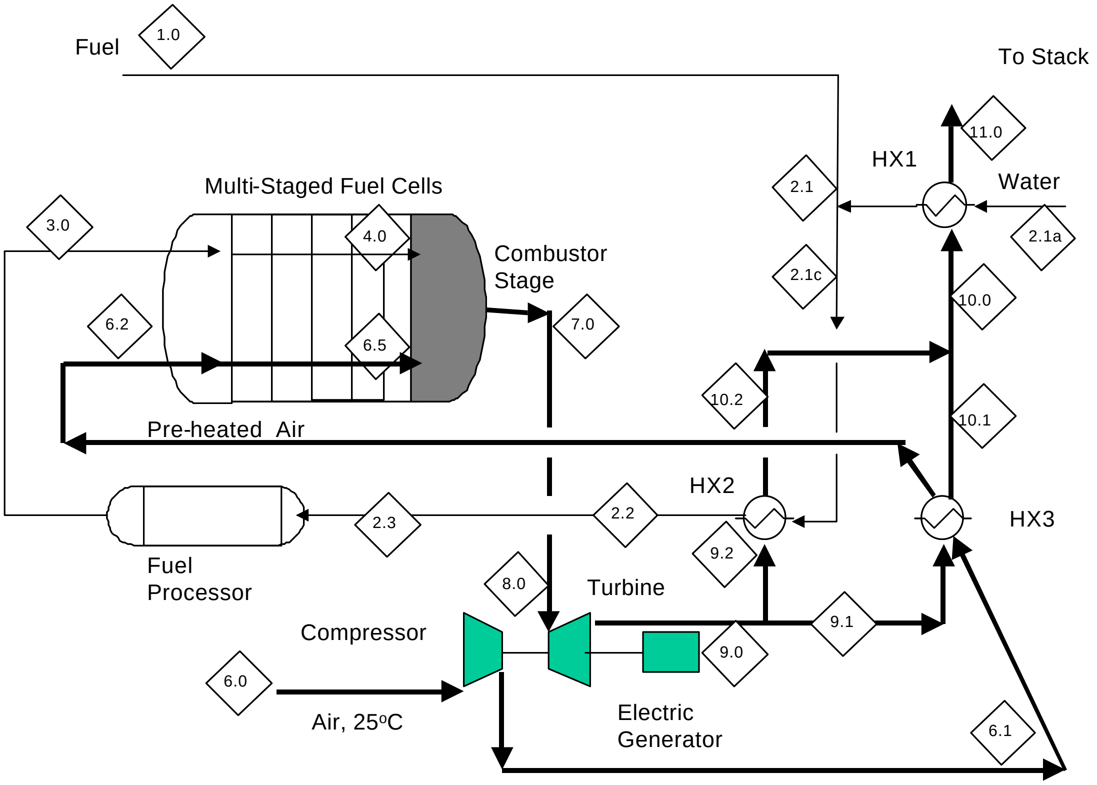

Figure 8. UltraFuelCell with gas turbine system.

We replaced the combustor stage with two SETS reactors that heat gases to the same temperature as the un-modified UltraFuelCell system. However, in the SETS there are two gas streams: one containing CO_2 and water vapor and the other containing N_2 and O_2, but no carbon dioxide. Two gas turbines, one in each of the two gas streams, are assumed to expand the gases to the same low pressure (17 psia) so that the net power in both the fuel cell and gas turbine are the same with and without SETS. However, after the water is condensed, the CO_2 must be compressed to pipeline pressure (assumed to be 750 psia, 51 atm). The compression of the CO_2 reduces the net power by only 2.3% of the 100% capture of the CO_2. Based on the cost of natural gas and the $3.22/kWh for electricity in the un-modified UltraFuelCell, the added efficiency cost of SETS is only $3.50/ton CO_2. Additional capital costs will be incurred for the SETS reactors, condensers, and CO_2 compressors (see Figure 9), raising the total for CO_2 capture to less than $5/ton CO_2.

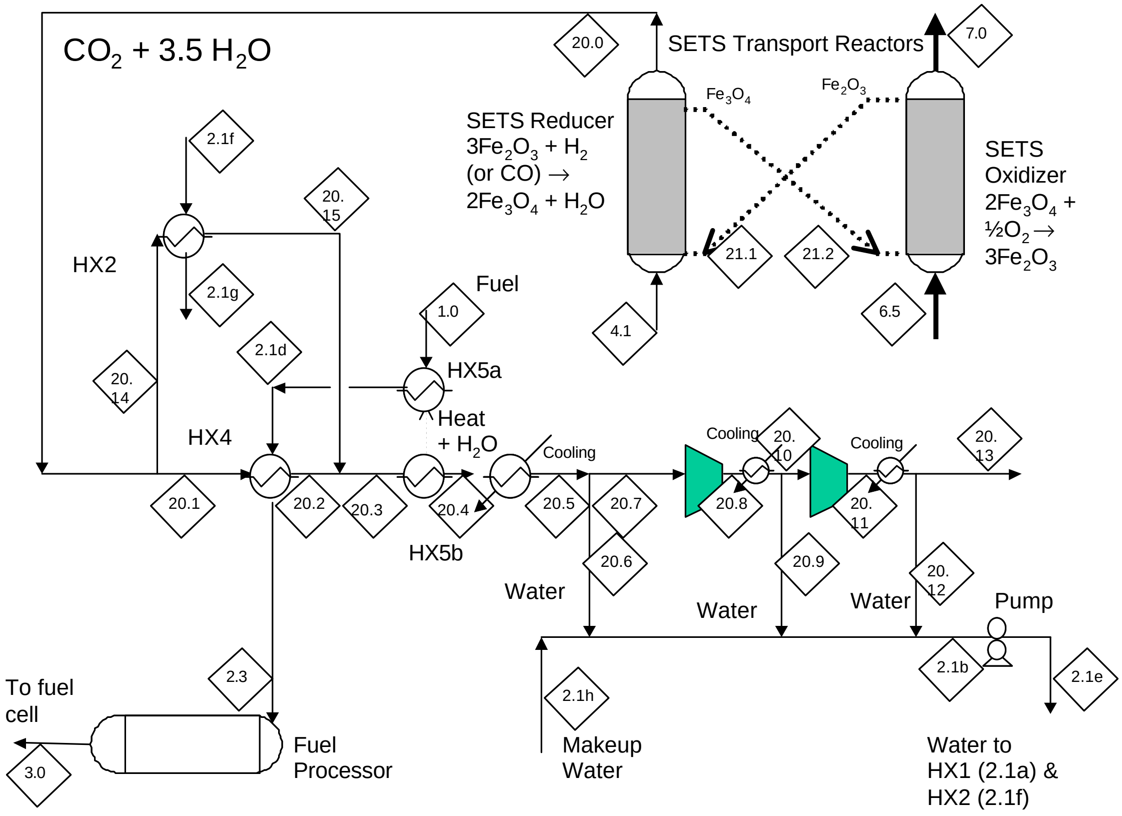

Figure 9. SETS components in an UltraFuelCell.

LSU Subcontract

Appendix A presents LSU's latest progress report summarizing current analysis results and planned future analyses. Changes were made in the base case simulations using both Cu-Fe and Fe-only sorbents to increase the sorbent circulation rates to 120% of stoichiometric (the previous sorbent circulation rate was 100% of stoichiometric). In addition, one standpipe was eliminated in the three-reactor configuration using Cu-Fe sorbent and the diameters of the remaining standpipes were decreased. A first round of estimates of purchased equipment costs and total capital requirement was completed for the Cu-Fe sorbent case. The estimated total capital requirement for the SETS process is $10.9 million, or just less than 10% of the base total capital estimate for the GE MS7001FA natural gas combined cycle plant.

Future Activities

We will continue to test our best formulations for chemical activity and durability, and conduct multiple cycle tests (up to 50) in the fluidized bed reactor on the most promising sorbents. We will also select one method of increasing CO_2 capture with SETS based on input from DOE.

LSU will complete its cost analyses and prepare its final report.

REFERENCES

s

Albans A.S. and M. Steinberg, *Environmental Control Technology for Atmospheric Carbon Dioxide*, DOE/EV-0079, Brookhaven National Laboratory, Brookhaven, NY (1980).

Egested, P.M. (1995). "Lightweight Ceramic Filter Components: Evaluation and Application" in *Proceedings of the Advanced Coal-Fired Power Systems '95 Review Meeting*, Morgantown, West Virginia: U.S. Department of Energy Morgantown Energy Technology Center, Report No. DOE/METC-95/1018 (DE95009732).

Herzog H., E. Drake, J. Tester and R. Rosenthal, *A Research Needs Assessment for the Capture, Utilization, and Disposal of Carbon Dioxide from Fossil Fuel-Fired Power Plants*, DOE/ER-30194, U.S. Department of Energy, Washington, DC (1993).

Herzog H.J. and E.M. Drake*, Long-Term Advanced CO2 Capture Options,* IEA/93/0E6, IEA Greenhouse Gas R&D Programme, Cheltenham, UK (1993).

Herzog H.J., E. Adams, D. Auerbach and J Caulfield, *Technology Assessment of CO2 Ocean Disposal*, Report 95-001, MIT Energy Laboratory, Cambridge, MA (1995).

Herzog, H. et al. (1996), *Energy Conv. Magmt*. 37, 999.

Ishida, M. and H. Jin (1994). *J. Chem. Engng. Japan*, 27, 296.

Ishida, M. et al. (1987). *Energy*, 20, 147.

Ishida. M. et al. (1996). *Energy and Fuels*, 10, 958.

Kirkpatrick, M. and R. Pike (1994). *AIChE Symposium Series*, Vol. 90, No. 298.

Lippert, T.D., G.J. Bruck, Z.N. Sanjana, and R.A. Newby. (1995). "Westinghouse Advanced Particle Filter System" in *Proceedings of the Advanced Coal-Fired Power Systems '95 Review Meeting*, Morgantown, West Virginia: U.S. Department of Energy Morgantown Energy Technology Center, Report No. DOE/METC-95/1018 (DE95009732).

Marchetti C, "On Geoengineering and the CO_2 Problem", *Climatic Change* 1(1), pp. 59-68 (1977).

Mimura T., H. Simayoshi, T. Suda, M. Iijima and S. Mituoka, "Development of Energy Saving Technology for Flue Gas Carbon Dioxide Recovery by Chemical Absorption Method and Steam System in Power Plant", *Energy Convers. Mgmt*., in press (1997).

Mudd, M.J. and J.D. Huffman (1993). "Initial Operation of the Tidd PFBC Hot Gas Clean Up Filter, *Advanced Coal-Fired Power Systems '93 Review Meeting*, Morgantown, WV: U.S. Department of Energy Morgantown Energy Technology Center, Report No. DOE/METC-93/6131 (DE93000289).

Richter, H. and K. Knoche (1983). In *Efficiency and Costing*, ACS Symposium Series 235.

Smelser, S. and G. Booras (1991). *Energy* 16, 1295.

Steinberg M., "Production of Hydrogen and Methanol from Natural Gas with Reduced CO Emission", *Hydrogen Energy Progress XI*, Proc. of the 11th World Hydrogen Energy Conf., Stuttgart, 1, pp. 499-510 (1996).

Steinberg M., *An Analysis of Concepts for Controlling Atmospheric Carbon Dioxide*,

Distribution:

File 2821
R. Copeland
M. Cesario
M. Dubovik

DOE-FETC

Technical Monitor: Thomas P. Dorchak
Project Manager
National Energy Technology Lab
U.S. Department of Energy
3610 Collins Ferry Road
P.O. Box 880
Morgantown, WV 26507-0880

Contracting Officer: Alexis W. Puher
Contract Manager
National Energy Technology Lab
U.S. Department of Energy
3610 Collins Ferry Road
P.O. Box 880
Morgantown, WV 26507-0880

Electronic copy to: National Energy Technology Lab
U.S. Department of Energy
Contractor Reports Receipt Coordinator
M/S F07
3610 Collins Ferry Road
P.O. Box 880
Morgantown, WV 26507-0880

Appendix A
LSU Progress Report for June 2000

ASPEN MODELING OF

A NOVEL CO_2 SEPARATION SYSTEM

Progress Report 10

By

Jinghan Yu
Armando B. Corripio
Douglas P. Harrison

Department of Chemical Engineering
Louisiana State University
Baton Rouge LA 70803

Submitted to

TDA Research, Inc.
12345 West 52nd Ave.

Wheat Ridge, CO 80033

June 2000

Overview

Changes were made in the base case simulations using both Cu-Fe and Fe-only sorbents to increase the sorbent circulation rates to 120% of stoichiometric (the previous sorbent circulation rate was 100% of stoichiometric). In addition, one standpipe was eliminated in the three-reactor configuration using Cu-Fe sorbent and the diameters of the remaining standpipes were decreased. A first round of estimates of purchased equipment costs and total capital requirement was completed for the Cu-Fe sorbent case. The estimated total capital requirement for the SETS process is $10.9 million, or just less than 10% of the base total capital estimate for the GE MS7001FA natural gas combined cycle plant.

Aspen Simulation

The complete stream material balances from the Aspen simulation using sorbent circulation rates of 120% of stoichiometric are attached. Simulation 45c (Table 1) represents the Cu-Fe sorbent and 47c (Table 2) represents the Fe sorbent.

Reactor Design

A diagram of the new two-standpipe configuration for the Cu-Fe sorbent is shown in Figure 1. In addition to eliminating one standpipe, the diameters of the remaining two were reduced. The diameter of the standpipe for reactor 3 was reduced from 6.7 m to 1 m and the standpipe for reactor 1 was reduced from 2.3 m to 0.2 m. These changes have only minimal effect on the economics since the standpipes do not contribute significantly to the total equipment cost. Other equipment dimensions were unchanged from the values reported last month.

Purchased Equipment Cost

Formulas used for estimating purchased equipment cost for the major items in the SETS process are summarized in Table 3. The applicable dates and sources for the cost estimate are also presented. All costs were updated to 1999 using the ratio of the cost index for 1999 (390.6) to the cost indices for the year given, and the final estimated costs figures are presented in Table 4.

The total capital requirement includes such items as equipment installation, utilities, engineering fees, working capital, and contingencies. The total capital requirement estimate of $10.9 million was determined using typical factors found in Peters and Timmerhaus. This value is just less than 10% of the reported total capital cost of the MS7001FA combined cycle plant.

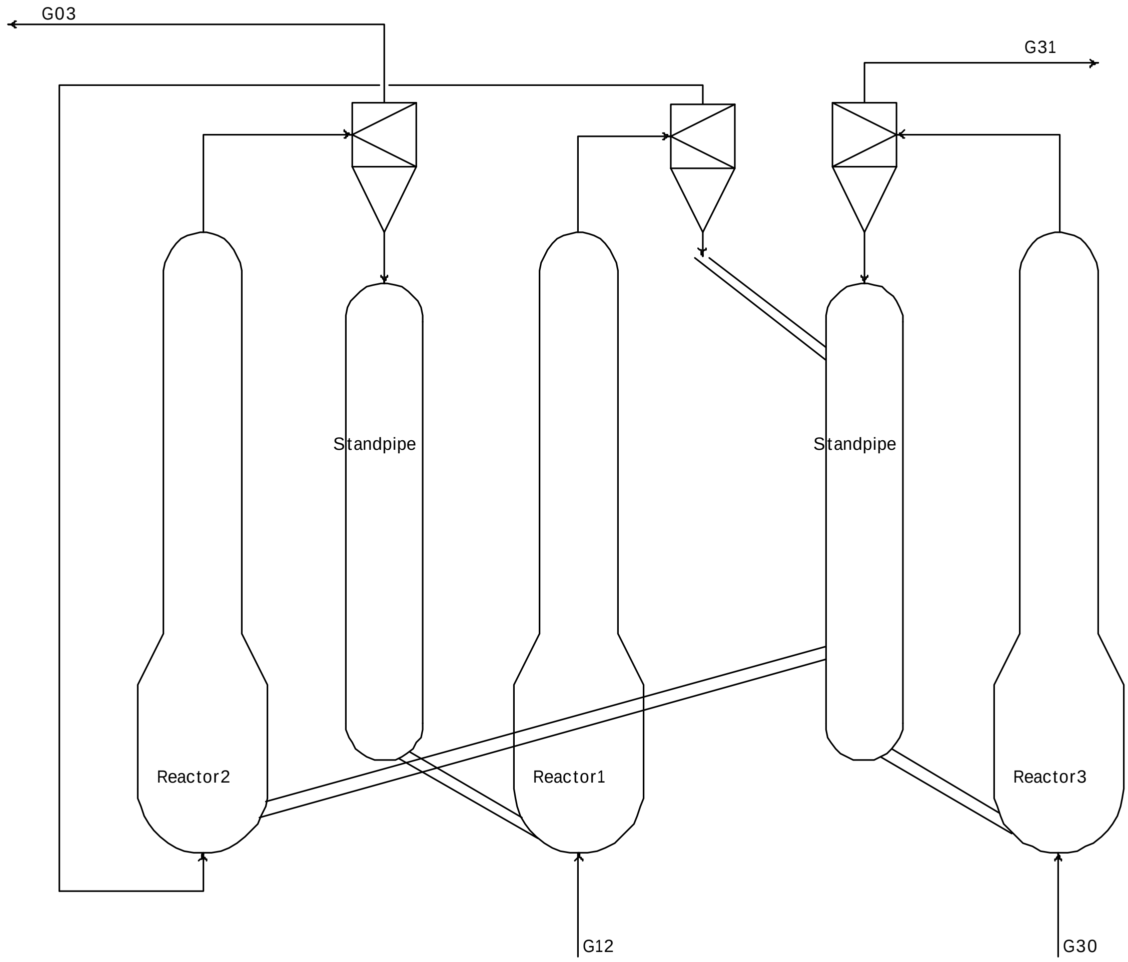

Figure 1. Schematic Configuration of The 3-Transport-Reactor System

Table 1. Simulation Results Of SETS System With Fe-Cu Sorbent

	G01	G02	G03	G04	G05	G06	G07	G08	G09	G10	G11	G12	G13	G14	G16	G17	G18	G19	G20
Temperature C	15	843	904.4	843	616	843	540	130	40	39.9	125.1	553.6	799.7	15	1287.6	589.4	559.8	496.8	468.3
Pressure bar	13.679	15.057	15.401	15.057	16.436	15.057	14.712	14.367	14.022	13.678	35.464	16.091	15.746	15.057	14.712	1.038	1.036	1.033	1.031
Vapor Frac	1	1	1	1	1	1	1	0.411	0.335	1	1	1	1	1	1	1	1	1	1
Mole Flow kmol/hr	964.17	2892.5	5785	5785	3856.7	2892.5	2892.5	2892.5	2892.5	968.22	968.22	4133.6	5784.1	998.27	53316	54768	54768	54768	54768
Mass Flow kg/hr	15468	77173	154345	154345	92641	77173	77173	77173	77173	42490	42490	92641	142004	16015	1E+06	2E+06	2E+06	2E+06	2E+06
Volume Flow cum/hr	1644.6	17851	36837	35702	17355	17851	13243	2715.8	1722.6	1732.2	848.72	17679	32830	1542.9	471602	4E+06	4E+06	3E+06	3E+06
Enthalpy MMkcal/hr	-17.299	-178.68	-353.32	-357.35	-195.98	-178.68	-188.19	-216.41	-223.08	-90.826	-90.122	-191.94	-314.74	-17.917	133.97	-175.79	-188.65	-215.69	-227.83
Mole Flow kmol/hr																			
CU																			
CUO																			
FEO																			
FE2O3																			
H2O		1928.3	3856.7	3856.7	1928.3	1928.3	1928.3	1928.3	1928.3	4.629	4.629	1731.3	3331.3		5402.6	5417.1	5417.1	5417.1	5417.1
O2		0.003	0.006	0.006	0.003	0.003	0.003	0.003	0.003	0.003	0.003				6859.3	7164.2	7164.2	7164.2	7164.2
CH4	964.17	trace	trace	trace	964.17	trace	trace	trace	trace			825.71	0.481	998.27					
CO2		964.17	1928.3	1928.3	964.17	964.17	964.17	964.17	964.17	963.58	963.58	1022.8	1682.9		998.26	998.26	998.26	998.26	998.26
N2															40055	41188	41188	41188	41188
AL2O3																			
H2		0.004	0.007	0.007	0.004	0.004	0.004	0.004	0.004	0.004	0.004	473.98	524.44		0.016	0.016	0.016	0.016	0.016
CO		0.002	0.005	0.005	0.002	0.002	0.002	0.002	0.002	0.002	0.002	79.876	244.97		0.008	0.008	0.008	0.008	0.008
C																			

	G21	G22	G23	G24	G25	G26	G27	G28	G29	G30	G31	G33	G34	G35	G36	G37	G38	G39	H01	H02
Temperature C	341	280.3	234.5	228.1	201	171.6	137.1	15	392.4	495.6	899.6	392.4	471.4	665.7	658.8	392.4	89.7	1285.6	497.7	833.1
Pressure bar	1.028	1.026	1.023	1.021	1.018	1.016	1.014	1.013	15.401	15.401	14.712	15.401	15.401	1.038	1.038	15.401	1.014	14.712	15.746	15.401
Vapor Frac	1	1	1	1	1	1	1	1	1	1	1	1	1	1	1	1	1	1	1	1
Mole Flow kmol/hr	54768	54768	54768	54768	54768	54768	54768	52805	52805	54246	52317	1452.1	51353	53316	54768	51353	54768	53316	2892.5	2892.5
Mass Flow kg/hr	2E+06	2E+06	2E+06	2E+06	2E+06	2E+06	2E+06	2E+06	2E+06	2E+06	1E+06	41750	1E+06	1E+06	2E+06	1E+06	2E+06	1E+06	52110	52110
Volume Flow cum/hr	3E+06	2E+06	2E+06	2E+06	2E+06	2E+06	2E+06	1E+06	190946	226373	348087	5251	207650	4E+06	4E+06	185695	2E+06	470991	11626	17252
Enthalpy MMkcal/hr	-280.93	-305.7	-324.15	-326.73	-337.57	-349.25	-362.92	-34.281	108.48	-10.194	151.88	2.983	135.93	-148.34	-145.36	105.49	-381.54	133.01	-155.63	-146.12
Mole Flow kmol/hr																				
CU																				
CUO																				
FEO																				
FE2O3																				
H2O	5417.1	5417.1	5417.1	5417.1	5417.1	5417.1	5417.1	528.05	528.05	3406.1	3406	14.521	513.53	5402.6	5417.1	513.53	5417.1	5402.6	2892.5	2892.5
O2	7164.2	7164.2	7164.2	7164.2	7164.2	7164.2	7164.2	11089	11089	10784	8855.8	304.95	10784	6859.3	7164.2	10784	7164.2	6859.3		
CH4																				
CO2	998.26	998.26	998.26	998.26	998.26	998.26	998.26							998.26	998.26		998.26	998.26		
N2	41188	41188	41188	41188	41188	41188	41188	41188	41188	40055	40055	1132.7	40055	40055	41188	40055	41188	40055		
AL2O3																				
H2	0.016	0.016	0.016	0.016	0.016	0.016	0.016				< 0.001			0.016	0.016		0.016	0.016		
CO	0.008	0.008	0.008	0.008	0.008	0.008	0.008							0.008	0.008		0.008	0.008		
C																				

	H03	H04	H05	H06	H07	H09	H10	H11	H12	H13	H14	H15	H16	H17	H18	H19	H20	H21	H22	H23
Temperature C	20	39.9	161.2	412.2	232.5	312.2	312.2	345.4	537.8	537.8	34.1	213.6	284.3	497.7	161.4	214.5	162.4	497.7	161.4	161.2
Pressure bar	6.55	13.678	6.205	103.77	6.205	104.11	104.11	6.205	20.339	103.42	0.04	20.684	20.684	15.746	21.029	104.46	104.8	15.746	21.029	6.205
Vapor Frac	0	0	0.72	1	1	1	0	1	1	1	0.865	0	1	1	0	0	0	1	0	0
Mole Flow kmol/hr	2892.5	1924.3	2892.5	9271	12433	9271	9270.9	9540.8	11442	9271	12433	2171	11442	11442	2171	9270.9	9270.9	8549.4	9270.9	1239.2
Mass Flow kg/hr	52109	34682	52109	167019	223990	167019	167017	171880	206130	167019	223990	39111	206130	206130	39111	167017	167017	154020	167017	22325
Volume Flow cum/hr	52.197	35.421	11709	4372.3	82403	3069.6	266.97	78175	37434	5643.7	7E+06	49.853	24229	45988	46.033	213.21	196.87	34362	196.58	26.269
Enthalpy MMkcal/hr	-199.99	-132.26	-171.76	-512.04	-697.8	-524.18	-577.28	-526.04	-611.56	-499.19	-735.99	-141.04	-638.6	-615.64	-143.62	-602.04	-612.88	-460	-613.32	-81.992
Mole Flow kmol/hr																				
CU																				
CUO																				
FEO																				
FE2O3																				
H2O	2892.5	1923.7	2892.5	9271	12433	9271	9270.9	9540.8	11442	9271	12433	2171	11442	11442	2171	9270.9	9270.9	8549.4	9270.9	1239.2
O2		trace																		
CH4																				
CO2		0.591																		
N2																				
AL2O3																				
H2		trace																		
CO		trace																		
C																				

	H24	H25	H26	H27	H28	H29	H30	H31	H32	H33	H34	H35	H36	H37	H38	H39	H40	H41	H42	H43
Temperature C	366.3	161.4	161.2	161.2	213.6	161.2	300.9	29.1	29.1	161.2	161.2	213.6	213.6	312.2	312.2	111	161.2	161.2	110.9	101
Pressure bar	6.205	21.029	6.205	6.205	20.684	6.205	20.684	0.04	1.379	6.205	6.205	20.684	20.684	104.11	104.11	6.55	6.205	6.205	1.379	1.379
Vapor Frac	1	0	0	0	1	1	1	0	0	0	1	0	1	0	1	0	1	1	0	0
Mole Flow kmol/hr	8549.4	11442	11442	12681	2171	1239.2	9271	12433	12433	1239.2	1239.2	2171	2171	9270.9	9270.9	12681	991.39	247.85	12681	12433
Mass Flow kg/hr	154020	206128	206128	228453	39111	22325	167019	223990	223990	22325	22325	39111	39111	167018	167018	228453	17860	4465	228453	223990
Volume Flow cum/hr	72509	242.61	242.55	268.82	3881.3	6961.5	20330	226.36	226.36	26.269	6961.5	49.853	3881.3	266.97	3069.6	252.11	5569.2	1392.3	252.1	244.31
Enthalpy MMkcal/hr	-469.79	-756.94	-757.04	-839.03	-122.59	-70.311	-516.01	-857.31	-857.3	-81.992	-70.31	-141.04	-122.59	-577.28	-524.17	-852.7	-56.249	-14.062	-852.73	-838.68
Mole Flow kmol/hr																				
CU																				
CUO																				
FEO																				
FE2O3																				
H2O	8549.4	11442	11442	12681	2171	1239.2	9271	12433	12433	1239.2	1239.2	2171	2171	9270.9	9270.9	12681	991.39	247.85	12681	12433
O2																				
CH4																				
CO2																				
N2																				
AL2O3																				
H2																				
CO																				
C																				

(Table Continued)

M01	M02	M03
904.4	799.7	899.6
15.401	15.746	14.712
1	1	1
5785.03	5784.063	52317.285
154345.13	142004.21	1466830
36836.76	32829.79	348086.97
-353.319	-314.736	151.884
3856.675	3331.277	3406.025
0.006		8855.816
trace	0.481	
1928.336	1682.891	
		40055.443
0.007	524.444	< 0.001
0.005	244.97	
1208320	1146620	5732100
-2570.234	-2408.83	-8870.108
904.4	799.7	899.6
15.401	15.746	14.712
0	0	0
9726.635	11609.025	37024.152
1053980	1004610	4265270
406.922	268.786	1743.272
-2216.914	-2094.095	-9021.993
300.739	1503.696	
1503.696	300.739	7217.74
941.195	4705.973	
2352.987	470.597	11294.336
4628.019	4628.019	18512.076

	S01	S02	S03	S04	S05	S06
Enthalpy MMkcal/hr	-2255.498	-2216.914	-2094.095	-6766.494	-8860.589	-9021.993
Temperature C	899.6	904.4	799.7	899.6	878.5	899.6
Pressure bar	14.712	15.401	15.746	14.712	15.057	14.712
Vapor Frac	0	0	0	0	0	0
Mole Flow kmol/hr	9256.038	9726.635	11609.025	27768.114	39377.138	37024.152
Mass Flow kg/hr	1066320	1053980	1004610	3198950	4203570	4265270
Volume Flow cum/hr	435.818	406.922	268.786	1307.454	1542.331	1743.272
Enthalpy MMkcal/hr	-2255.498	-2216.914	-2094.095	-6766.494	-8860.589	-9021.993
Mole Flow kmol/hr						
CU		300.739	1503.696		1503.696	
CUO	1804.435	1503.696	300.739	5413.305	5714.044	7217.74
FEO		941.195	4705.973		4705.973	
FE2O3	2823.584	2352.987	470.597	8470.752	8941.349	11294.336
H2O						
O2						
CH4						
CO2						
N2						
AL2O3	4628.019	4628.019	4628.019	13884.057	18512.076	18512.076
H2						
CO						
C						

	Q01	Q02
QCALC MMkcal/hr	4.034102	30.435274

	W01	W02	W03	W04	W05	W06
POWER kW	-320663.4	166022.12	819.55215	-43533.89	-4643.727	-11152.52
	W07	W08	W09	W10	W11	
POWER kW	-19179.06	9.3544929	110.96831	508.25978	40.234877	

Power Generated kW	399172.58
Power Consumed kw	167510.49
Simple Cycle Power kW	154641.26
Net Power kW	231662.09
HHV Efficiency	0.4772972
LHV Efficiency	0.5296632

Table 2 Simulation Results Of SETS System With Fe-only Sorbent

	G01	G02	G03	G04	G05	G06	G07	G08	G09	G10	G11	G12	G14	G15	G16	G17	G18	G19	G20	G21
Temperature C	15	843	875.5	843	616	843	540	130	40	39.9	122.8	535.7	15	872.3	1288	589.4	559.8	496.8	468.2	340.7
Pressure bar	13.679	15.401	15.746	15.401	16.436	15.401	15.057	14.712	14.367	14.022	35.464	16.091	15.057	14.712	14.712	1.038	1.036	1.033	1.031	1.028
Vapor Frac	1	1	1	1	1	1	1	0.409	0.335	1	1	1	1	1	1	1	1	1	1	1
Mole Flow kmol/hr	968.297	2904.89	5809.79	5809.79	3873.19	2904.89	2904.89	2904.89	2904.89	972.281	972.281	4109.9	998.546	53320	53320	54772.2	54772.2	54772.2	54772.2	54772.2
Mass Flow kg/hr	15534.2	77501.9	155004	155004	93036.1	77501.9	77501.9	77501.9	77501.9	42669.6	42669.6	93036.1	16019.4	1482810	1482810	1524560	1524560	1524560	1524560	1524560
Volume Flow cum/hr	1651.68	17526.6	35294	35053.2	17428.9	17526.6	12994.4	2649.68	1686.46	1693.94	845.946	17187.9	1543.32	346532	471767	3784430	3663080	3394040	3275930	2719330
Enthalpy MMkcal/hr	-17.373	-179.44	-356.74	-358.88	-196.81	-179.44	-188.99	-217.4	-224.04	-91.21	-90.524	-194.67	-17.921	133.456	133.463	-176.54	-189.41	-216.48	-228.63	-281.79
Mole Flow kmol/hr																				
CU																				
CUO																				
FEO																				
FE2O3																				
H2O		1936.56	3873.12	3873.12	1936.56	1936.56	1936.56	1936.56	1936.56	4.552	4.552	1760.81		3418.43	5415.5	5430.02	5430.02	5430.02	5430.02	5430.03
O2		trace	< 0.001	< 0.001	trace	trace	trace	trace	trace	trace	trace			8847.59	6850.51	7155.46	7155.46	7155.46	7155.46	7155.46
CH4	968.297				968.297							849.942	998.546	998.546						
CO2		968.275	1936.55	1936.55	968.275	968.275	968.275	968.275	968.275	967.668	967.668	1025.66			998.537	998.538	998.538	998.538	998.538	998.538
N2														40055.4	40055.4	41188.1	41188.1	41188.1	41188.1	41188.1
AL2O3																				
H2		0.038	0.075	0.075	0.038	0.038	0.038	0.038	0.038	0.038	0.038	412.492		< 0.001	0.016	0.016	0.016	0.016	0.016	0.016
CO		0.022	0.045	0.045	0.022	0.022	0.022	0.022	0.022	0.022	0.022	60.989			0.009	0.008	0.008	0.008	0.008	0.008
C																				

	G22	G23	G24	G25	G26	G27	G28	G29	G30	G31	G33	G34	G35	G36	G37	G38	G39	H01	H02	H03
Temperature C	280	234.2	227.7	200.6	171.2	136.6	15	392.4	496	900	392.4	471.7	666	659.1	392.4	89.2	1286	497.7	833.2	20
Pressure bar	1.026	1.023	1.021	1.018	1.016	1.014	1.013	15.401	15.401	14.712	15.401	15.401	1.038	1.038	15.401	1.014	14.712	15.746	15.401	6.55
Vapor Frac	1	1	1	1	1	1	1	1	1	1	1	1	1	1	1	1	1	1	1	0
Mole Flow kmol/hr	54772.2	54772.2	54772.2	54772.2	54772.2	54772.2	52805.3	52805.3	54258	52321.5	1452.15	51353.1	53320	54772.2	51353.1	54772.2	53320	2904.89	2904.89	2904.89
Mass Flow kg/hr	1524560	1524560	1524560	1524560	1524560	1524560	1518170	1518170	1528760	1466790	41749.8	1476420	1482810	1524560	1476420	1524560	1482810	52332.4	52332.4	52332.5
Volume Flow cum/hr	2456050	2258010	2234750	2118720	1991940	1841130	1248160	190946	226547	348229	5251.02	207744	4010930	4090100	185695	1627780	471154	11675.6	17327	52.42
Enthalpy MMkcal/hr	-306.59	-325.06	-327.64	-338.49	-350.19	-363.88	-34.281	108.475	-10.684	151.377	2.983	136.06	-148.95	-145.97	105.492	-382.52	132.505	-156.3	-146.74	-200.84
Mole Flow kmol/hr																				
CU																				
CUO																				
FEO																				
FE2O3																				
H2O	5430.03	5430.03	5430.01	5430.01	5430.01	5430.03	528.053	528.053	3418.42	3418.43	14.521	513.531	5415.5	5430.02	513.531	5430.03	5415.5	2904.89	2904.89	2904.89
O2	7155.46	7155.46	7155.46	7155.46	7155.46	7155.46	11089.1	11089.1	10784.2	8847.59	304.95	10784.2	6850.51	7155.46	10784.2	7155.46	6850.51			
CH4																				
CO2	998.538	998.538	998.538	998.538	998.538	998.538							998.538	998.538		998.538	998.538			
N2	41188.1	41188.1	41188.1	41188.1	41188.1	41188.1	41188.1	41188.1	40055.4	40055.4	1132.67	40055.4	40055.4	41188.1	40055.4	41188.1	40055.4			
AL2O3																				
H2	0.016	0.016	0.016	0.016	0.016	0.016				< 0.001			0.016	0.016		0.016	0.016			
CO	0.008	0.008	0.008	0.008	0.008	0.008							0.008	0.008		0.008	0.008			
C																				

	H04	H05	H06	H07	H09	H10	H11	H12	H13	H14	H15	H16	H17	H18	H19	H20	H21	H22	H23	H24
Temperature C	39.9	161.2	412.2	232.7	312.2	312.2	345.3	537.8	537.8	34.1	213.6	284.3	497.7	161.4	214.5	162.4	497.7	161.4	161.2	366.3
Pressure bar	14.022	6.205	103.766	6.205	104.11	104.11	6.205	20.339	103.421	0.04	20.684	20.684	15.746	21.029	104.455	104.8	15.746	21.029	6.205	6.205
Vapor Frac	0	0.722	1	1	1	0	1	1	1	0.865	0	1	1	0	0	0	1	0	0	1
Mole Flow kmol/hr	1932.61	2904.89	9281.22	12447.1	9281.22	9281.24	9542.2	11454.6	9281.22	12447.1	2173.4	11454.6	11454.6	2173.4	9281.24	9281.24	8549.72	9281.24	1240.61	8549.72
Mass Flow kg/hr	34832.3	52332.5	167204	224238	167204	167204	171905	206358	167204	224238	39154.3	206358	206358	39154.3	167204	167204	154026	167204	22349.9	154026
Volume Flow cum/hr	35.574	11793.7	4377.12	82521.4	3073	267.27	78184.2	37475.9	5649.97	6872770	49.909	24255.8	46039.2	46.084	213.45	197.093	34363.7	196.798	26.299	72511.6
Enthalpy MMkcal/hr	-132.83	-172.44	-512.61	-698.55	-524.76	-577.92	-526.12	-612.24	-499.74	-736.8	-141.2	-639.31	-616.32	-143.78	-602.72	-613.57	-460.02	-614.01	-82.083	-469.8
Mole Flow kmol/hr																				
CU																				
CUO																				
FEO																				
FE2O3																				
H2O	1932.01	2904.89	9281.22	12447.1	9281.22	9281.24	9542.2	11454.6	9281.22	12447.1	2173.4	11454.6	11454.6	2173.4	9281.24	9281.24	8549.72	9281.24	1240.61	8549.72
O2	trace																			
CH4																				
CO2	0.607																			
N2																				
AL2O3																				
H2	trace																			
CO	trace																			
C																				

	H25	H26	H27	H28	H29	H30	H31	H32	H33	H34	H35	H36	H37	H38	H39	H40	H41	H42	H43
Temperature C	161.4	161.2	161.2	213.6	161.2	300.9	29.1	29.1	161.2	161.2	213.6	213.6	312.2	312.2	111	161.2	161.2	110.9	101
Pressure bar	21.029	6.205	6.205	20.684	6.205	20.684	0.04	1.379	6.205	6.205	20.684	20.684	104.11	104.11	6.55	6.205	6.205	1.379	1.379
Vapor Frac	0	0	0	1	1	1	0	0	0	1	0	1	0	1	0	1	1	0	0
Mole Flow kmol/hr	11454.6	11454.6	12695.2	2173.39	1240.61	9281.22	12447.1	12447.1	1240.6	1240.6	2173.39	2173.39	9281.2	9281.2	12695.2	992.484	248.121	12695.2	12447.1
Mass Flow kg/hr	206358	206358	228708	39154.2	22349.8	167204	224238	224238	22349.8	22349.8	39154.2	39154.2	167203	167203	228708	17879.9	4469.97	228708	224238
Volume Flow cum/hr	242.883	242.817	269.116	3885.63	6969.19	20352.1	226.609	226.61	26.298	6969.25	49.908	3885.63	267.269	3073.01	252.39	5575.35	1393.84	252.379	244.58
Enthalpy MMkcal/hr	-757.79	-757.88	-839.97	-122.73	-70.389	-516.58	-858.26	-858.25	-82.083	-70.388	-141.2	-122.73	-577.92	-524.75	-853.65	-56.311	-14.078	-853.69	-839.61
Mole Flow kmol/hr																			
CU																			
CUO																			
FEO																			
FE2O3																			
H2O	11454.6	11454.6	12695.2	2173.39	1240.61	9281.22	12447.1	12447.1	1240.6	1240.6	2173.39	2173.39	9281.2	9281.2	12695.2	992.484	248.121	12695.2	12447.1
O2																			
CH4																			
CO2																			
N2																			
AL2O3																			
H2																			
CO																			
C																			

(Table Continued)

M2	M3
875.5	900
15.746	14.712
1	1
5809.785	52321.462
155003.84	1466790
35293.974	348228.96
-356.739	151.377
3873.115	3418.427
< 0.001	8847.593
1936.55	
	40055.443
0.075	< 0.001
0.045	
3741400	16060200
-7740.081	-30030.24
875.5	900
15.746	14.712
0	0
24013.837	111547.87
3586390	14593400
976.868	7108.979
-7383.342	-30181.62
2324.094	55773.934
13943.484	55773.934

	S1	S3	S4	S5	S6
Mass Flow kg/hr	3648360	3586390	10945100	14531500	14593400
Enthalpy MMkcal/hr	-7545.405	-7383.342	-22636.22	-30019.56	-30181.62
Temperature C	900	875.5	900	894.8	900
Pressure bar	14.712	15.746	14.712	15.057	14.712
Vapor Frac	0	0	0	0	0
Mole Flow kmol/hr	27886.967	24013.837	83660.901	107674.74	111547.87
Mass Flow kg/hr	3648360	3586390	10945100	14531500	14593400
Volume Flow cum/hr	1777.245	976.868	5331.734	6267.076	7108.978
Enthalpy MMkcal/hr	-7545.405	-7383.342	-22636.22	-30019.56	-30181.62
Mole Flow kmol/hr					
CU					
CUO					
FEO					
FE2O3	13943.484	2324.094	41830.45	44154.544	55773.934
H2O					
O2					
CH4					
CO2					
N2					
AL2O3	13943.484	13943.484	41830.45	55773.934	55773.934
H2					
CO					
C					
FE3O4		7746.26		7746.26	

	Q1	Q2
QCALC MMkcal/hr	2.1398383	30.567788

	W01	W02	W03	W04	W05	W06
POWER kW	-320784.7	166022.12	798.02348	-43588.95	-4648.868	-11152.92
	W07	W08	W09	W10	W11	
POWER kW	-19200.3	9.3648604	111.09234	508.82784	40.279846	

Power Generated kW	399375.71
Power Consumed kw	167489.71
Simple Cycle Power kW	154762.56
Net Power kW	231886.01
HHV Efficiency	0.4766897
LHV Efficiency	0.5289891

Table 3. References for Purchased Equipment Cost Estimates

Unit	Formula	Source
Reactor	$\$80\left(\frac{Weight}{1lb}\right)^{0.66}$	Peters, 1991
Cyclone	$\$7{,}000\left(\frac{Output\,volume\;flow\,rate}{4.7\,m^3/s}\right)^{0.66}$	Perry, 1994
Heat Exchangers	$\$398\left(\frac{Heat\,Transfer\,Area}{1\,ft^2}\right)^{0.65}\left(F_d+F_p\right)F_m$, where F_d=1, F_p=0.1, F_m=1	Baasel, 1990
Air Compressor	$\$1{,}570\left(\frac{Power\;Input}{1\,hp}\right)^{0.82}$	Baasel, 1990
Insulation	$\text{Area} \times \$411.3/\text{m}^2$	Zhang, 1996

Table 4. SETS Purchased Equipment Cost Estimates

Unit	**Purchased Cost**	**Year**	**Index**	**1999 Cost**
Reactor 1	116,000	1990	356	127,000
Reactor 2	138,000	1990	356	151,000
Reactor 3	558,000	1990	356	612,000
REFORMER	38,000	1987	323.8	46,000
HRSG1	206,000	1987	323.8	248,000
RECUPER	304,000	1987	323.8	367,000
CO_2 Compressor	548,000	1987	323.8	661,000
Ejector	1,500	1963	102.4	6,000
Total				2,213,000

References:

1. Baasel, W. D. *Preliminary Chemical Engineering Design*. 1990. Van Nostrand Reinhold, New York.
2. Perry, R. H.; Chilton, C. H.; Kirkpatrick, S. D. *Chemical Engineers' Handbook*. 1994. McGraw-Hill.
3. Peters, M. S.; Timmerhaus, K. D. *Plant Design And Economics For Chemical Engineers*. 1991. McGraw-Hill.
4. Zhang, S. *Simulation And Economic Evaluation Of Elemental Sulfur Recovery From Hot Gas Desulfurization Processes*. 1996. Master's Thesis.